Sensing and Bio-Sensing Research 38 (2022) 100541

Contents lists available at ScienceDirect

Sensing and Bio-Sensing Research

journal homepage: www.elsevier.com/locate/sbsr

Application of metal oxide semiconductor for detection of ammonia emissions from agricultural sources

Bastiaan Molleman [a], Enrico Alessi [b], Dominika Krol [a], Phoebe A. Morton [c], Karen Daly [a,*]

[a] Teagasc, The Irish Agriculture and Food Authority, Johnstown Castle, Wexford Y35TC97, Ireland
[b] ST Microelectronics, Str. Primosole 50, 95121 Catania, CT, Italy
[c] Agri-Food and Biosciences Institute, 18a Newforge Lane, Belfast BT9 5PX, Ireland

ARTICLE INFO

Keywords:
Ammonia
Agriculture
Emission
Sensor
Metal-oxide semiconductor
Calibration

ABSTRACT

Agricultural emissions of ammonia (NH3) reduce air quality and biodiversity. Measuring the effectiveness of mitigations measures requires rapid monitoring tools, however, conventional methods are labour intensive and costly. This study evaluated the performance of a prototype metal oxide semiconductor (MOS) gas sensor for monitoring NH3. Conventional methods were used to calibrate sensor conductance. The metal oxide semiconductor (MOS) gas sensor was calibrated against NH3 released from a 0.1 M phosphate buffer spiked with ammonium chloride and NH3 released from recently spread cattle slurry. Field measurements using the MOS sensor were compared with values measuring a Bruker Open Path Air Monitoring System. Sensor conductance and NH3 concentration were described using single site Langmuir adsorption model. Field calibrations suggest a higher detection limit above 0.1 ppm and coefficients of determination were 0.93 and 0.89 for sensors 1 and 2, respectively. For prototypes deployed under field conditions, sensitivities of 2.2 and 2.4 with nonlinearity constants of 0.53 and 0.51, were found for sensor 1 and 3 respectively. Average R2 values were 0.88 for sensor 1 and 0.92 for sensor 3. The calibrations were used to calculate NH3 concentrations from slurry emissions using MOS sensor conductance. NH3 concentrations between 0.2 and 1 ppm, were measured with standard deviation of 20% of verified concentrations. The MOS sensor is sensitive enough to detect NH3 emission from agricultural sources with concentrations above 0.2 ppm. Low power and cost of MOS sensors are an advantage over existing techniques.

1. Introduction

Agricultural emissions of gaseous ammonia (NH_3) reduce air quality and biodiversity due to acidification and eutrophication of surrounding land and surface water [12]. Nitrogen losses due to ammonia volatilization after fertilization with organic or artificial fertilizer can be 30% or higher [2,24,25]. In addition to the environmental cost, this may represent a substantial financial cost for farmers, both in wasted resources and in decreased production. Ammonia emissions also cause indirect greenhouse gas emissions as ammonia that is deposited on soil is partly emitted as nitrous oxide (N_2O) [3]. Finally, ammonia emissions contribute to formation of fine particulate matter which is associated with a range of adverse health effects [6,8]. Monitoring is an important tool in increasing our understanding of emissions and mitigations measures. It should be obvious, therefore, that adequate monitoring of gaseous ammonia concentrations is vital from an environmental, economic and social perspective.

Ammonia emissions from soil can be analysed by adsorbing gaseous ammonia into an acidic liquid phase which is later analysed for ammonia content. This core concept can be applied in a variety of experimental set-ups, such as wind tunnels [13], in the open field [26], and in closed and vented chambers [27]. These methods are labour intensive and costs quickly escalate if a high sampling frequency is required. The absorption generally takes place over hours or longer to attain measurable quantities, leading to a considerable loss of resolution. Moreover, a considerable lag time can exist between collecting a sample and obtaining the results. Direct measurement of gas concentrations could reduce labour, increase resolution and facilitate fast intervention measures.

Direct measurement of gas concentrations is possible with a variety of more recent technologies. Advances in laser technology, such as the quantum cascade laser, and cavity ring down spectroscopy have enabled

* Corresponding author.
E-mail address: karen.daly@teagasc.ie (K. Daly).

https://doi.org/10.1016/j.sbsr.2022.100541
Received 11 August 2022; Received in revised form 25 October 2022; Accepted 17 November 2022
Available online 21 November 2022
2214-1804/© 2022 The Authors. Published by Elsevier B.V. This is an open access article under the CC BY-NC-ND license (http://creativecommons.org/licenses/by-nc-nd/4.0/).

extremely low detection limits down to the sub ppb level [14,17]. Alternatively, photoacoustic spectroscopy (PAS) can detect concentrations down to ±3 ppb, using cantilever enhanced PAS [7]. However, while power consumption has reduced drastically, long-term in-situ monitoring requires considerable upkeep. Moreover, commercially available solutions are expensive and are not suited for multi-site roll out.

Metal oxide semiconductor (MOS) sensors are a cheap and low power alternative for gas sensing. In MOS gas sensors, gases interact with the metal oxide surface and either donate or accept electrons, depending on the type of sensor and the type of gas [5]. This changes the electrical conductivity of the sensor material, which is continuously measured. The technology is mature, having been the subject of continuous research for over forty years [5,15,29], and has been shown to yield stable measurements over long periods of time even under harsh conditions [4]. This makes MOS sensors a potentially suitable candidate for high temporal and spatial monitoring of emissions from agriculture.

MOS sensors exhibit excellent sensitivity to ammonia, concentrations as low as 0.5 ppm have shown to give a very clear response [18]. Both ZnO [16,18,21,22] and SnO_2 [20] have been used as sensing material. MOS sensors are non-selective, which is considered to be one of the main limiting factors to their widespread use. However, the literature reports a much higher sensitivity to ammonia than for other gases that have been tested. The relatively high sensitivity to ammonia suggests that interference by other gases may be limited, despite the non-selective nature of MOS sensors.

The objective of this study was to evaluate the performance of a prototype MOS gas sensor manufactured by ST Microelectronics for detection and monitoring of ammonia emissions from agricultural sources. We performed two field calibrations: under semi-controlled conditions in a dynamic chamber, and under uncontrolled conditions in the open atmosphere. The results from these calibrations were used to evaluate the sensitivity and selectivity of the gas sensor for ammonia in the context of monitoring emissions from agriculture.

2. Material and methods

In this work, the GHT25 metal oxide semiconductor gas sensor prototype, manufactured by ST Microelectronics, was evaluated for use as a selective ammonia sensor. Sensor material consisted of tin oxide (SnO_2) nanomaterial deposited over a micro hotplate, which heated up the sensor material to operating temperature. The internal redox reaction occurs at 350 °C by the micro hot plate to deposit the sensor material. The sensor is optimized to operate within the temperature range − 20 to 85 °C. The heater current could be run continuously for maximum sensitivity or intermittently for reduced power consumption. As the focus in this work was on environmental monitoring, power consumption was an important consideration. We therefore used an intermittent heater profile of 0.1 s on, 1 s off, which had been tested by STM to give a good balance of sensitivity and power consumption.

Calibrations were performed under field conditions using two sets of calibrations, with laboratory made solutions and cow slurry as the respective sources of ammonia. The sources of ammonia were tested in different experimental set-ups, schematically shown in Fig. 1. In every experiment, two different sensors were run simultaneously: sensors 1 and 2 in the calibrations using ammonia from synthetic solutions, and, because sensor 2 broke down, sensors 1 and 3 in the calibrations using ammonia from cow slurry.

In the experiments using a synthetic ammonia source, ambient air was fed through a modified head-space chamber of 10 cm height, and a surface area of 0.25 m^2, which was placed in a paddock of perennial ryegrass. In passing over the soil and grass, the air picked up potential gaseous emissions. However, in order to facilitate a calibration over a wider range of concentrations, an additional ammonia source was integrated into the experiment. Thus, the main function of the head-space chamber was to enrich the airstream with contaminants and to ensure compatibility with future work.

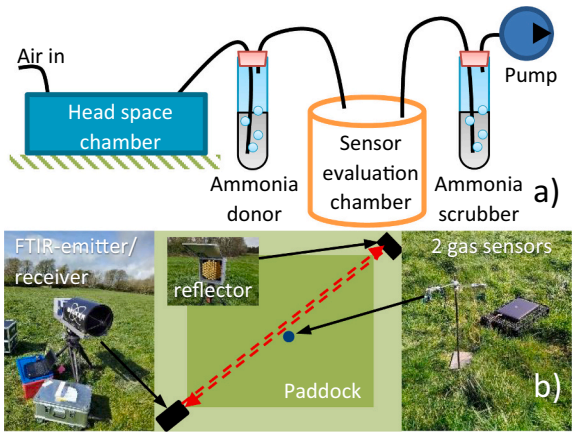

Fig. 1. Schematic representation of the experimental set-up used for the calibrations using (a) synthetic ammonia, and (b) ammonia from slurry. In the experiments using ammonia from solution, air flowed into the head-space chamber, and from there through the ammonia donor solution, the sensor evaluation chamber, and the ammonia scrubber solution. Experiments using slurry were performed in the open air, with the sensors placed in a paddock shortly after slurry spreading, off to the side of the infrared beam (shown as a red dotted line). (For interpretation of the references to colour in this figure legend, the reader is referred to the web version of this article.)

The air from the head-space chamber was bubbled through 100 mL of 0.1 M $K_{1.5}H_{1.5}PO_4$ solution, having a pH of 7.2 at standard conditions, which was spiked with ammonium chloride. The buffered ammonium chloride solution released gaseous ammonia into the airstream at a rate which was modified by changing the concentration of ammonium chloride and was calculated to decrease at most by 3% per hour (see Fig. S1), which was acceptable for our purposes. Calculations are detailed in the supplementary information.

The ammonia enriched air was led to a chamber containing two sensors, and finally bubbled through a scrubbing solution, consisting of 100 mL dilute (0.02 M) phosphoric acid, in which gaseous ammonia redissolved as NH_4^+. Stiff PTFE tubing was used to connect all vessels within the system and a vacuum pump, calibrated daily to within 1% of 2 L/min over a 10-min time span was placed at the air outlet to provide the airflow. Ammonium concentrations in the phosphoric acid were determined by a certified laboratory, which performed spectroscopic analysis using an Aquakem 600A (Thermo Scientific), after converting ammonium to monochloramine and reacting with salicylate in presence of nitroprusside [1]. Using the flowrate of air, an average concentration of gaseous ammonia was calculated for the time-interval the ammonia was collected.

Each experimental run allowed between 1 and 2 h for concentrations to stabilize, as the sensor signal suggested that concentrations of gaseous ammonia kept rising during this time. This was a result of ammonia adsorption to the internal surfaces of the system and is unfortunately unavoidable at low concentrations. When the signal had stabilized, the ammonia scrubber solution was refreshed, and ammonia was collected for exactly 1 h. The scrubber solutions used during stabilization were not analysed.

In the experiments with ammonia from slurry, the sensors were placed in a recently (1 to 5 days) spread paddock in which atmospheric ammonia concentrations were monitored using a Bruker-OPS (Open Path Air Monitoring System) from Bruker Optik GmbH. The spectrometer emits modulated radiation in the infrared spectral range. This radiation is focused by the telescope onto a distant retroreflector array which reflects the radiation back, through the telescope onto the MCT-Detector of the spectrometer. The infrared beam was directed diagonally across the paddocks and gas sensors were placed slightly off centre in the paddock (see Fig. 1b), at the approximate height of the IR beam.

Data were collected at three separate spreading events in March, June, and August of 2021. The March and June experiments took place at Teagasc in Johnstown Castle, Co. Wexford, Republic of Ireland; the August experiment at AFBI in Loughgall, Co. Armagh, Northern Ireland. Aerated and non-aerated slurry was used, and slurry was spread using splash plate, trailing hose, trailing shoe, and injection on different paddocks. No distinction is made in the data analysis between location, season, slurry type and spreading technique.

To account for fluctuations in ammonia concentrations due to wind and turbulence, and inherent differences between a point measurement as made by the gas sensor and a field average as measured by the open path IR beam, data was averaged over intervals of 60 min. In some cases, shorter intervals were used where data collection was interrupted due to equipment malfunctioning or shut down due to adverse ambient conditions (e.g. rain). Where possible, exactly the same interval was used for the MOS sensor and the FTIR, except for the background measurements, which were sometimes taken at different times.

3. Linking sensor output to ammonia concentrations

The objective of these calibrations was to link sensor output to a concentration of the target gas, in this case ammonia. While the sensor signal was in the form of resistance (R), this was converted into conductance ($G = R^{-1}$), as the link with gas concentration is more intuitive.

The interaction of a reducing gas such as ammonia with an n-type semiconductor introduces electrons into the boundary layer, resulting in an increase in conductance ΔG. The conductance of an n-type semiconductor G_S ($\Omega^{-1} = S = C\,V^{-1}\,s^{-1}$) is determined by the number density n (m^{-3}), electrical charge e (C), and mobility μ ($m^2\,V^{-1}\,s^{-1}$) of electrons in the boundary layer and the effective cross-section A (m^2) and length ℓ (m) of the conductive boundary layer, according to:

$$G_S = ne\mu\frac{A}{\ell} \tag{1}$$

This implies that, as long as electron mobility is not affected by increased electron density, the increase in conductance will be proportional to the amount of introduced electrons. Assuming an equal number of electrons x is donated for every adsorbed ammonia molecule, the change in conductance can thus be expressed as:

$$\Delta G = Q \bullet SSA \bullet N_A \bullet xe\mu\frac{A}{\ell} \tag{2}$$

where Q (mol m^{-2}) is the amount of ammonia adsorbed to the sensor, SSA is the specific surface area ($m^2\,m^{-3}$) of the boundary layer, and N_A is the Avogadro constant (mol^{-1}).

The sensor conductance can be then expressed as a function of adsorption:

$$G_S = G_0 + \Delta G = G_0 + fQ \tag{3}$$

where G_0 is the conductance in background air and f ($C\,m^2\,mol^{-1}\,V^{-1}\,s^{-1}$) is a constant equal to $SSA \bullet N_A \bullet xe\mu \bullet A/\ell$. Assuming the simplest adsorption reaction, the relationship between gas adsorption Q and gas concentration C (μmol mol^{-1} = ppm) can be described with a single site Langmuir adsorption model [11]:

$$Q = Q_{max}\frac{KC}{1+KC} \tag{4a}$$

where Q_{max} is the adsorption maximum (mol m^{-2}) and K is the equilibrium constant (no units). This expression may be expanded with a coefficient a to account for non-ideal behaviour [9], yielding:

$$Q = Q_{max}\frac{KC^a}{1+KC^a} \tag{4b}$$

Under conditions of low site saturation, defined as $KC^a << 1$, Eq. (4b) simplifies to

$$Q = Q_{max}KC^p \tag{4c}$$

Substituting Q in Eq. (3a) gives:

$$G_S = G_0 + SC^p = G_0(1+\bar{S}C^p) \tag{5}$$

with S equal to $fQ_{max}K$, and $\bar{S} = S/G_0$.

Eq. (5) can be rearranged to $G_S/G_0 = R_0/R_S = 1 + \bar{S}C^n$, which is identical to the general expression for gas sensor response $R_0/R_S = 1 + AC$ [5], except for the coefficient a. A coefficient has also been applied elsewhere in the literature to describe gas sensor response [10,16,23].

4. Results and discussion

The objective of this study was to evaluate the use of MOS sensors for detection of ammonia emissions from agriculture. Various studies on MOS sensors have reported a much higher response to ammonia than to other gases tested on the same sensor [16,18,20–22]. A secondary objective was to investigate if that high sensitivity would extend to a quasi-selectivity under agricultural conditions. To fulfil these objectives, we performed two calibrations: using atmospheric air with ammonia from a controlled synthetic source, and using atmospheric air with ammonia emitted from cow slurry.

4.1. Calibrations with synthetic ammonia

In a typical experiment, the sensor signal took around an hour to stabilize after initiating the gas flow or increasing the concentration of ammonium chloride in the donor solution (see Fig. S2). The apparent sluggish response of the sensor was a consequence of gas adsorption to the internal surfaces of the set-up, and could not be avoided despite using chemically inert PTFE tubing and reducing tube length as much as possible.

Once the signal had stabilized, the system was left running for one hour. The sensor signal obtained during this time was averaged and is

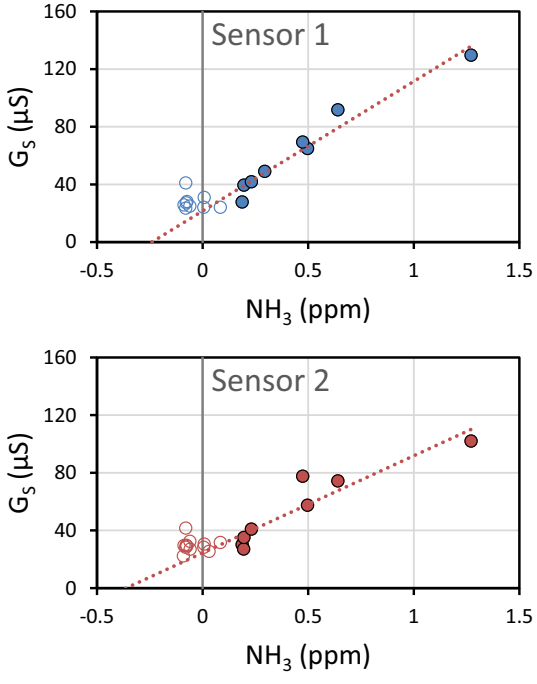

Fig. 2. Sensor calibration data generated using sensor conductance (G_S) and a synthetic ammonia (NH_3) source. Unfilled datapoints had a verified ammonia concentration less than the uncertainty of the validation method (0.1 ppm) and were not used in the derivation of the model parameters.

plotted in Fig. 2 against the average concentration of gaseous ammonia, which was calculated from the concentration of dissolved ammonia in the scrubber solution.

The analysis of ammonia concentration in the scrubber solution resulted in a large number of negative concentrations, equivalent to concentrations of gaseous ammonia of up to −0.1 ppm. This unexpected result is not understood, but it suggests an uncertainty of at least ±0.1 ppm in the ammonia concentrations. For derivation of model parameters, we therefore only included data points with an ammonia concentration >0.1 ppm.

The data in Fig. 2 have been described using Eq. (5). Under controlled conditions, the preferred approach was to determine the value of G_0, after which S^- and a were found via linear regression using a double logarithmic plot of $\Delta G/G_0 = G_S/G_0 - 1$ against C. However, the uncontrolled conditions encountered in the field were not conducive for determining an unambiguous value for the background conductance. We therefore applied an optimization, whereby G_0, was varied and the resulting parameters S^- and a were evaluated. The optimization criterion was to give the highest average coefficient of determination (R^2) value based on predictions of both conductance data (G_S) and the logarithm of relative conductance increase ($\Delta G/G_0$). This approach mitigated an overly strong influence on the fit of both high concentration data points, of which there were few, and low concentration data points, which were highly variable.

The above approach resulted in a non-ideality coefficient $a > 1$. This is not supported by adsorption theory and is therefore considered an artefact. The non-ideality coefficient was set to unity, which reduces Eq. (2) to a linear equation. Linear regression was applied to the data to find G_0 and S^-, which were 22 and 4.2, respectively, for sensor 1, and 24 and 2.8, respectively, for sensor 2. The R^2 for all data points, including those with $NH_3 < 0.1$ ppm, were 0.93 and 0.89 for sensors 1 and 2, respectively. Negative concentrations were set to zero for the calculations of R^2.

Sensor 1 performed much better than Sensor 2 when verified (i.e., measured in the scrubber solution) ammonia concentrations over 0.1 ppm were compared to those calculated from sensor conductance of G_0 and S^- by linear regression. The difference between predicted and verified concentrations, expressed as a percentage of the verified concentration was 4% on average with a standard deviation of 25%, for Sensor 1, and 10 ± 44% for Sensor 2.

Data at concentrations below 0.1 ppm were excluded from the current data analysis, as the accuracy of the verification data was below expectation. Assuming for simplicity that no gaseous ammonia was present in these runs, we can use the sensor data obtained to gain some insight on variability of the background sensor signal G_0. The conductance values of these low concentration data points showed a large scattering, averaging 28 ± 5 μS for Sensor 1 and 30 ± 5μS for Sensor 2. The predicted ammonia concentrations calculated from these conductance values, where the verified ammonia concentrations were below 0.1 ppmI, using their respective calibration parameters were 0.06 ppm on average with a standard deviation of 0.07 ppm for sensor 1 and 0.08 ± 0.07 ppm for sensor 2. It suggests that, for these sensors, a detection limit of around 0.2 ppm might be appropriate. The detection limit will be further discussed in the next section.

4.2. Calibrations with ammonia from cattle-slurry

In the experiments with cattle-slurry ammonia, both the sensor signal and the ammonia concentrations measured by FTIR spectrometer varied strongly within the 60-min measurement intervals used, as shown in Fig. S3 of the supplementary information. These variations reflect fluctuations in the ammonia concentrations due to changing wind speeds and localized eddy phenomena. As the correlation between data points within an interval was weak, the average values of all data points within each interval were used for our data analysis.

Fig. 3 shows the average MOS conductance for the two sensors

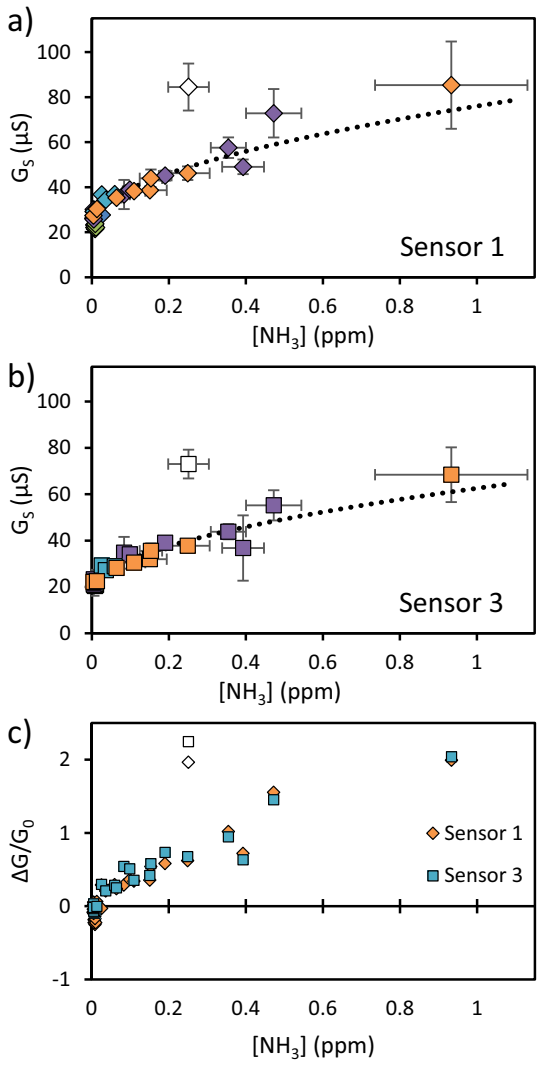

Fig. 3. Conductance (G_S) of (a) Sensor 1 and (b) Sensor 3, and (c) relative conductance increase ($\Delta G/G_0$) for both sensors plotted against ammonia (NH_3) concentrations as determined using open path FTIR laser spectroscopy. Data points represent averages of data collected over variable time intervals; error bars represent 1 standard deviation of the concentration or conductance recorded in these intervals. Dotted lines represent models as described with Eq. (2) using $G_0 = 24.1$, $S^- = 2.15$, and $a = 0.53$ for Sensor 1 and $G_0 = 18.2$, $S^- = 2.44$, and $a = 0.51$ for Sensor 3. The relative conductance increase for both sensors is calculated as $\Delta G/G_0 = G_S/G_0 - 1$. The open symbols deviate strongly due to interference and were excluded from the fit.

plotted against average ammonia concentrations as measured by FTIR open path spectrometry. In general, a positive correlation between conductance and ammonia concentration was observed. The background measurements, which were taken from an untreated upwind location, show the presence of between 3 and 14 ppb of ammonia and a conductance between 20 and 30 μS on sensor 1 and between 20 and 24 μS for sensor 3. The correlation is very weak ($R^2 > 0.05$), as shown in Fig. S4 of the supplementary information, which could suggest that other factors dominate sensor response at these low concentrations.

For both sensors, a single data point deviated strongly from the correlation (unfilled data point in Fig. 3), which was collected within the first hour after spreading. A short-lived spike in conductance and emission peaks of one or more additional gases immediately after spreading may explain the deviation from the overall trend. None of the other gases that were measured using FTIR (CH_4, CO, H_2O) showed a strong, short-lived increase in concentrations which could have

explained this deviation and these can therefore be excluded as the cause. This interference may be caused by volatile fatty acids, aromatic compounds or reduced sulphur compounds, which show short-lived emission peaks after application of slurry or manure [19,28]. Therefore, this point was not included in fitting the model parameters to the data.

Data was well-described using Eq. (2), with optimized background conductance values of 24.1 μS for sensor 1 and 18.2 μS for sensor 3. Respective sensitivities of 2.2 and 2.4 were found, and non-linearity constants of 0.53 and 0.51. Average R^2 values, i.e. the average of R^2 for the fit of G_S and R^2 for the fit of $\log(\Delta G/G_0)$, were 0.88 for sensor 1 and 0.92 for sensor 3. For sensor 1, six data points were encountered which had a value below the fitted background conductance of 24.1 μS. All of these datapoints were collected on the same day, at low ammonia concentrations (8 ± 2 ppb). On that day, no data above 24.1 μS was registered by sensor 1. Moreover, while the average ratio between data points for sensors 1 and 3 was 0.8 ± 0.05, for these datapoints, a ratio of 0.95 was found. The reason for these aberrations is not clear. In our derivation of parameters, these datapoints could not be included as $\Delta G/G_0$ was negative, however, they were included in the calculating the R^2 of the predicted conductance value G_S.

An even better fit was obtained with respective background conductance values of 28.5 and 22.5 for sensors 1 and 3. Respective values for S^- and a were 2.1 and 0.76 for sensor 1 and 2.0 and 0.69 for sensor 3. In this case, however, almost half of the data points, including all datapoints obtained in March, were below G_0 for both sensors. The resulting negative value for $\Delta G/G_0$ excluded these data from the dataset used to derive parameters. The two very different fits imply that the fitting parameters are useful to describe observed data, but care is needed about using them to predict measurements outside of the data range investigated.

For both fits, a different background conductance was obtained for the two sensors. Moreover, the response to ammonia was apparently different. However, the sensor sensitivity S^- was very similar in both fits and for both sensors, while the non-linearity parameter a, differed between fits, but was quite similar between sensors. The similarities between the sensors become apparent when the relative increase in conductance is plotted, as shown in Fig. 3c for $G_0 = 24.1$ and 18.5. A similar pattern was observed when the other fit results $G_0 = 28.5$ and 22.5 were used. The similar behaviour when measurements were normalized to the background behaviour was striking, and could indicate that despite differences in the sensor material, sensor behaviour is determined by the same reactions. Note however, that these similarities in S^- were not found for sensor 2. Further research is needed to explore this phenomenon.

While the model description of the data was excellent, there were deviations. In the concentration range below 50 ppb, the predicted concentrations were between 4 times lower and 3.5 times higher than measured concentrations. Between 50 ppb and 1 ppm, MOS predictions were up to 1.6 times lower and 2 times higher than FTIR measurements. Nevertheless, in the latter range the average ratio between measured and predicted concentrations was 1, with a standard deviation of 0.3. Taking into consideration that averaged data was plotted over a period with high fluctuations, as shown in Fig. S3, and that field averages (FTIR) were compared to point measurements (MOS), the agreement between predictions and measured concentrations is excellent.

4.3. Comparing synthetic ammonia data and slurry ammonia data

Sensor 1 was used both in the calibration with synthetic ammonia and with slurry, which allowed a detailed look at sensor behaviour under these two different conditions. A very different set of model parameters was derived using the synthetic ammonia data than using the slurry data: an overview of parameters obtained for sensor 1 is given in Table 1. The background conductance was slightly lower, while the sensitivity parameter S^- was nearly double that used for the slurry calibration compared to the synthetic ammonia calibration. The most striking difference, however, was the values for a, being 1 and 0.57, indicating a completely different behaviour. We note, however, that the value for a became more apparent over concentrations ranging orders of magnitude, which was not the case in the synthetic ammonia calibrations.

Table 1
Fitted parameters for describing ammonia response for sensor 1, using data collected in calibrations with synthetic ammonia and with ammonia from cattle slurry, as well as all data pooled. Two fits are shown for the slurry data, the second fit having a higher R^2, but omitting many data points.

Data-set	G_0	S^-	a
synthetic ammonia data	21.6	4.2	1[a]
slurry data – fit 1	24.7	2.2	0.57
slurry data – fit 2	28.5	2.0	0.73
Pooled data	29.0	2.3	0.86

[a] Fixed to 1 (see Section 4.1).

While large differences were observed in the fitted parameters, calibration data for the two set-ups were in surprisingly good agreement. Synthetic ammonia data and slurry data are plotted together in Fig. 4. When the optimization of G_0 was performed for the pooled data, an excellent result was obtained for G_0 of 28.9, with resulting values for S^- and a being 2.4 and 0.89, and an average of $R^2 = 0.93$. At this high background conductance, many low concentration data points were omitted from the derivation of S^- and a, explaining why a was so close to 1. A second optimum was found at $G_0 = 25.3$, with $S = 2.2$ and $a = 0.66$, but the average coefficient of determination was considerably worse with $R^2 = 0.82$.

A recurring observation in these fits is that the trend changes substantially when low concentration data are omitted. The reason for these different results cannot be identified with certainty using the data obtained in the current work. An explanation could be that the non-selective nature of MOS sensors picks up variations in other gases when ammonia concentrations are low. Alternatively, our model may be too simple, being loosely based on low saturation adsorption to a single type of surface site. A high affinity site with low surface density, and a low affinity site with high surface density would lead to different response curves at low and high ammonia concentrations. This, however, is outside of the scope of the current work.

4.4. Implications for environmental monitoring

One of the objectives of the current study was to evaluate these prototype MOS sensors for environmental monitoring of ammonia. To investigate this, the calibration parameters, obtained using synthetic ammonia, were applied to the sensor data obtained in the open-field after slurry spreading. These “sensed” ammonia concentrations were

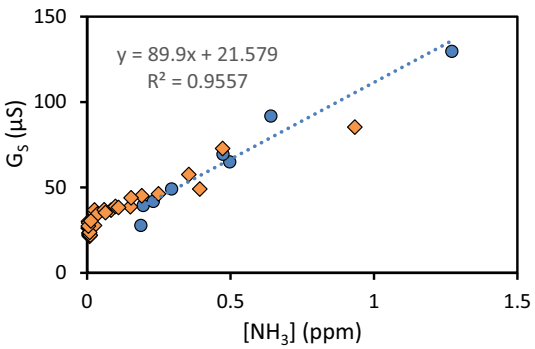

Fig. 4. Calibration data for sensor 1 obtained in the calibration using synthetic ammonia (diamonds) and in calibration using slurry ammonia (circles), fitted with a single model.

plotted against FTIR measurements, as shown in Fig. 5. Ammonia concentrations as determined by the MOS sensor showed a slight positive bias and were overestimated at low concentration as a result of the difference in G_0 and a. However, at concentrations above 0.1 ppm, the agreement between predictions and measurement strongly improved. Between 0.1 and 1 ppm, the predicted concentration averaged 1.2 ± 0.3 times the measured concentration; between 0.2 and 1 ppm, this improved to 1.0 ± 0.2 times the measured concentration.

These results indicated that the MOS sensor is sensitive enough to detect ammonia emission from agricultural soils after slurry spreading. The results further suggest that concentrations can be reliably determined above 0.2 ppm, which the FTIR data unequivocally show can realistically be encountered in the field. Applicability of the MOS sensor for ammonia detection may be further expanded in combination with a set-up to contain and concentrate emissions, such as a head−space accumulator. Wang et al. [27] reported ammonia emissions of up to 7, 87, and 517 g/ha/d in soil fertilized with 0, 60 and 120 kg of urea-N, in a closed chamber set-up. These values are equivalent to 0.25, 3.2 and 19 ppm after 30 min in a standard 10 cm head-space gas accumulator. These data suggest that even unfertilized soil can emit ammonia at levels measurable by the MOS sensor when used in conjunction with a head-space chamber.

5. Conclusions

This work evaluated the sensitivity of a MOS based gas sensor to measure emissions of gaseous ammonia in an agricultural setting. Calibrations were performed using synthetic ammonia from a donor solution in semi-controlled conditions. Untreated atmospheric air was drawn over a patch of perennial ryegrass at a fixed flow rate, but with no active measures to prevent interference from other gases, temperature or humidity control. Additionally, the sensors were tested in the open atmosphere after slurry spreading in three different seasons. In both cases, the correlation between sensor conductance and ammonia concentration could be described using single site Langmuir adsorption models. An optimization was applied to find the background conductance, which is not easily established outside of a carefully controlled laboratory setting. While a different set of parameters was found for the two experiments, calibration data were very comparable, showing both the limitations of the applied model and the reproducibility of the sensor. Large deviations from the model line were found in the first hour after spreading, suggesting the presence of an unidentified interferent gas. More research is required to investigate if conditions for deviating data can be established. The calibrations with synthetic ammonia were used to calculate ammonia concentrations in the slurry experiment, based on sensor conductance. In the range between 0.2 and 1 ppm, ammonia concentrations were correctly predicted, with a standard deviation of 20% of the verified concentrations. This result can be viewed as suggesting that these sensors behave as selective indicators for ammonia under environmental conditions, except immediately after spreading. The results suggest that the ST MOS gas sensors evaluated in this work, have a strong potential for environmental monitoring of agricultural emissions. While the concentration range for reliable measurement is considerably less sensitive than state-of-the-art technology (e.g. FTIR), the low power consumption and cost of MOS sensors are considerable advantages over existing techniques. The application of MOS sensors could enable monitoring for long periods at remote locations due to a considerable reduction in costs, labour and energy requirements. These advantages would facilitate monitoring at a much higher frequency and density. It is clear that this technology has potential for environmental monitoring of gaseous ammonia emissions from agriculture and targeting of measures to reduce them.

Funding

This work was supported by the European Union's Horizon 2020 Research and Innovation Programme [grant agreement No. 825325].

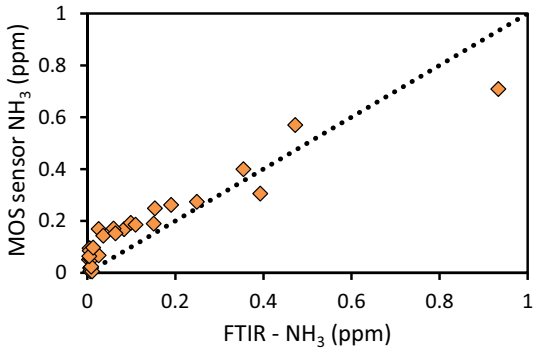

Fig. 5. Ammonia concentrations after slurry spreading as calculated using Sensor 1 conductance measurements plotted against FTIR measurements. MOS sensor ammonia concentrations were calculated using model parameters derived from calibration data obtained using synthetic ammonia (Fig. 2).

Declaration of Competing Interest

The authors declare that they have no known competing financial interests or personal relationships that could have appeared to influence the work reported in this paper.

Data availability

Data will be made available on request.

Acknowledgements

We gratefully acknowledge the help of David Kelleghan in sharing with us his keen expertise on ammonia emissions, which was of great value in the establishment of the work outlined in this paper.

Appendix A. Supplementary data

Supplementary data to this article can be found online at https://doi.org/10.1016/j.sbsr.2022.100541.

References

[1] Analysts, S.C, Ammonia in Waters 1981: Methods for the Examination of Waters and Associated Materials, Her Majesty's Stationary Office, London, 1982.
[2] M. Carozzi, R.M. Ferrara, G. Rana, M. Acutis, Evaluation of mitigation strategies to reduce ammonia losses from slurry fertilisation on arable lands, Sci. Total Environ. 449 (2013) 126–133.
[3] H. Denier van der Gon, A. Bleeker, Indirect N2O emission due to atmospheric N deposition for the Netherlands, Atmos. Environ. 39 (2005) 5827–5838, https://doi.org/10.1016/j.atmosenv.2005.06.019.
[4] W. Eugster, J. Laundre, J. Eugster, G.W. Kling, Long-term reliability of the Figaro TGS 2600 solid-state methane sensor under low-Arctic conditions at Toolik Lake, Alaska, Atmos. Meas. Tech. 13 (2020) 2681–2695, https://doi.org/10.5194/amt-13-2681-2020.
[5] G.F. Fine, L.M. Cavanagh, A. Afonja, R. Binions, Metal oxide semi-conductor gas sensors in environmental monitoring, Sensors 10 (2010) 5469–5502, https://doi.org/10.3390/s100605469.
[6] E. Giannakis, J. Kushta, A. Bruggeman, J. Lelieveld, Costs and benefits of agricultural ammonia emission abatement options for compliance with European air quality regulations, Environ. Sci. Eur. 31 (2019) 1–13.
[7] M. Guo, K. Chen, Z. Gong, Q. Yu, Trace Ammonia detection based on near-infrared Fiber-optic cantilever-enhanced photoacoustic spectroscopy, Photon. Sens. 9 (2019) 293–301, https://doi.org/10.1007/s13320-019-0545-x.
[8] S. Guthrie, S. Giles, F. Dunkerley, H. Tabaqchali, A. Harshfield, B. Ioppolo, C. Manville, The Impact of Ammonia Emissions from Agriculture on Biodiversity, RAND Corp. R. Soc, Cambridge, UK, 2018.
[9] T. Hiemstra, W.H. van Riemsdijk, Biogeochemical speciation of Fe in ocean water, Mar. Chem. 102 (2006) 181–197, https://doi.org/10.1016/j.marchem.2006.03.008.
[10] Y.V. Kaneti, X. Jiang, A. Yu, Controllable Synthesis of ZnO Nanoflakes with PDF, 2013.

[11] I. Langmuir, The adsorption of gases on plane surfaces of glass, mica and platinum, J. Am. Chem. Soc. 40 (1918) 1361–1403.
[12] A. Leip, G. Billen, J. Garnier, B. Grizzetti, L. Lassaletta, S. Reis, D. Simpson, M. A. Sutton, W. De Vries, F. Weiss, H. Westhoek, Impacts of European livestock production: nitrogen, Sulphur, phosphorus and greenhouse gas emissions, land-use, water eutrophication and biodiversity, Environ. Res. Lett. 10 (2015), 115004, https://doi.org/10.1088/1748-9326/10/11/115004.
[13] D.R. Lockyer, A system for the measurement in the field of losses of ammonia through volatilisation, J. Sci. Food Agric. 35 (1984) 837–848, https://doi.org/10.1002/jsfa.2740350805.
[14] S. Maithani, S. Mandal, A. Maity, M. Pal, M. Pradhan, High-resolution spectral analysis of ammonia near 6.2 μm using a cw EC-QCL coupled with cavity ring-down spectroscopy, Analyst 143 (2018) 2109–2114.
[15] H. Meixner, U. Lampe, Metal oxide sensors, Sensors Actuators B Chem. 33 (1996) 198–202, https://doi.org/10.1016/0925-4005(96)80098-0.
[16] G.H. Mhlongo, D.E. Motaung, F.R. Cummings, H.C. Swart, S.S. Ray, A highly responsive NH3 sensor based on Pd-loaded ZnO nanoparticles prepared via a chemical precipitation approach, Sci. Rep. 9 (2019) 1–18, https://doi.org/10.1038/s41598-019-46247-z.
[17] D.J. Miller, K. Sun, L. Tao, M.A. Khan, M.A. Zondlo, Open-path, quantum cascade-laser-based sensor for high-resolution atmospheric ammonia measurements, Atmos. Meas. Tech. 7 (2014) 81–93.
[18] A. Nancy Anna Anasthasiya, R.K. Kampara, P.K. Rai, B.G. Jeyaprakash, Gold functionalized ZnO nanowires as a fast response/recovery ammonia sensor, Appl. Surf. Sci. 449 (2018) 244–249, https://doi.org/10.1016/j.apsusc.2017.11.072.
[19] D.B. Parker, J. Gilley, B. Woodbury, K.-H. Kim, G. Galvin, S.L. Bartelt-Hunt, X. Li, D.D. Snow, Odorous VOC emission following land application of swine manure slurry, Atmos. Environ. 66 (2013) 91–100.
[20] R. Peng, Y. Li, T. Liu, Q. Sun, P. Si, L. Zhang, L. Ci, Reduced graphene oxide/SnO2@ au heterostructure for enhanced ammonia gas sensing, Chem. Phys. Lett. 737 (2019), 136829.
[21] M. Poloju, N. Jayababu, M.V.R. Reddy, Improved gas sensing performance of Al doped ZnO/CuO nanocomposite based ammonia gas sensor, Mater. Sci. Eng. B 227 (2018) 61–67.
[22] R. Sankar Ganesh, M. Navaneethan, V.L. Patil, S. Ponnusamy, C. Muthamizhchelvan, S. Kawasaki, P.S. Patil, Y. Hayakawa, Sensitivity enhancement of ammonia gas sensor based on Ag/ZnO flower and nanoellipsoids at low temperature, Sensors Actuators B Chem. 255 (2018) 672–683, https://doi.org/10.1016/j.snb.2017.08.015.
[23] R.W.J. Scott, S.M. Yang, G. Chabanis, N. Coombs, D.E. Williams, G.A. Ozin, Tin dioxide opals and inverted opals: near-ideal microstructures for gas sensors, Adv. Mater. 13 (2001) 1468–1472, https://doi.org/10.1002/1521-4095(200110)13:19<1468::AID-ADMA1468>3.0.CO;2-O.
[24] J.R. Soares, H. Cantarella, M.L. de Campos Menegale, Ammonia volatilization losses from surface-applied urea with urease and nitrification inhibitors, Soil Biol. Biochem. 52 (2012) 82–89.
[25] C. Tian, X. Zhou, Z. Ding, Q. Liu, G. Xie, J. Peng, X. Rong, Y. Zhang, Y. Yang, M. A. Eissa, Controlled-release N fertilizer to mitigate ammonia volatilization from double-cropping rice, Nutr. Cycl. Agroecosyst. 119 (2021) 123–137.
[26] R. Vandré, J. Clemens, H. Goldbach, M. Kaupenjohann, NH3 and N2O emissions after landspreading of slurry as influenced by application technique and dry matter-reduction. I. NH3 emissions, J. Plant Nutr. Soil Sci. 160 (1997) 303–307, https://doi.org/10.1002/jpln.19971600226.
[27] Z.H. Wang, X.J. Liu, X.T. Ju, F.S. Zhang, S.S. Malhi, Ammonia volatilization loss from surface-broadcast urea: comparison of vented- and closed-chamber methods and loss in winter wheat-summer maize rotation in North China plain, Commun. Soil Sci. Plant Anal. 35 (2004) 2917–2939, https://doi.org/10.1081/CSS-200036499.
[28] B. Woodbury, J.E. Gilley, D.B. Parker, D.B. Marx, D.N. Miller, R.A. Eigenberg, Emission of Volatile Organic Compounds after Land Application of Cattle Manure, 2014.
[29] N. Yamazoe, J. Fuchigami, M. Kishikawa, T. Seiyama, Interactions of tin oxide surface with O2, H2O AND H2, Surf. Sci. 86 (1979) 335–344, https://doi.org/10.1016/0039-6028(79)90411-4.